Single-cell RNA sequencing suggests plasmids constrain bacterial heterogeneity and conjugation is subpopulation specific

Valentine Cyriaque (valentinecyriaque@gmail.com)
University of Copenhagen https://orcid.org/0000-0002-2254-2690
Rodrigo Ibarra-Chávez
University of Copenhagen https://orcid.org/0000-0002-9056-3055
Anna Kuchina
Institute for Systems Biology
Georg Seelig
University of Washington
Joseph Nesme
University of Copenhagen
Jonas Madsen
University of Copenhagen https://orcid.org/0000-0003-4830-1796

Article

Keywords: Bacterial population heterogeneity, Single-cell transcriptomics, Plasmids, Conjugation, IncP-1, Pseudomonas putida KT2440

Posted Date: October 11th, 2023

DOI: https://doi.org/10.21203/rs.3.rs-3405585/v1

Additional Declarations: There is **NO** Competing Interest.

Single-cell RNA sequencing suggests plasmids constrain bacterial heterogeneity and conjugation is subpopulation specific

Valentine Cyriaque[1,2,*], Rodrigo Ibarra-Chávez[1], Anna Kuchina[3,4], Georg Seelig[4], Joseph Nesme[1], Jonas Stenløkke Madsen[1,*]

[1]Section of Microbiology, University of Copenhagen, Denmark
[2]Section of Proteomics and Microbiology, University of Mons, Belgium
[3]Institute for Systems Biology, Seattle, WA, USA
[4]Department of Electrical and Computer Engineering, University of Washington, Seattle, WA, USA
*Corresponding authors

Abstract

Transcriptional heterogeneity is common within isogenic bacterial populations. Nonetheless, the interplay between conjugative plasmids and host subpopulation dynamics remains elusive. Here, the efficacy of microbial split-pool ligation transcriptomics in unraveling plasmid-host interactions was demonstrated through the generation of high-quality single-cell transcriptomic data. We found that transcription was impacted by growth state but also by plasmid carriage at the single-cell level, resulting in a reduction in subpopulations. Transcriptional heterogeneity among plasmid-encoded genes was also uncovered. This included core plasmid functions such as replication and maintenance fluctuations, likely associated with the cell cycle. Other key heterogeneously transcribed functions included *tra* genes revealing a subpopulation not engaging in conjugation and representing a possible plasmid strategy decreasing its burden at the population level. In sum, this study advances the understanding of plasmid-mediated subpopulation dynamics through a comprehensive single-cell transcriptomics approach, providing valuable insights into the intricate interplay between plasmids and bacteria.

Key words

Bacterial population heterogeneity, Single-cell transcriptomics, Plasmids, Conjugation, IncP-1, *Pseudomonas putida* KT2440

Introduction

To survive and reproduce, bacteria perform numerous tasks, including importing and processing nutrients and metabolites, cell division, defense/resistance, exogenous DNA acquisition, and many others. Yet, the number of tasks is limited by intracellular competition for relevant resources[1]. Transcriptional heterogeneity at the single-cell level, resulting in subpopulations[2], expands the number of simultaneous processes that can be performed and can, for example, facilitate division of labor where complementary metabolic processes are carried out by different subpopulations[3]. Heterogeneity also enables bet-hedging strategies where mal-adapted phenotypes may become an asset in a changing environment[4]. The formation of subpopulations can thus increase the fitness of bacteria while preserving the genotype. Subpopulations arise in isogenic populations through epigenetic heritable determination[2], which emerges through a number of processes such as methylation[5], compartmentalization[6], and stochasticity during gene expression[1]. This results in transcriptionally and phenotypically distinct subpopulations[7] fluctuating over space and time and has been shown to be important for utilization of different metabolic substrates[1] and/or survival of an upcoming stress (*e.g.,* using detoxification[3], competence[8] or antibiotic persistence[9]).

Recently, several techniques successfully enabled single-cell transcriptomics in bacteria either by transcriptome imaging (Par-seq[10]), physically separating the cells with fluorescence-activated cell sorting (MATQ-seq[11,12]) or using random molecular-barcode ligation to concomitantly tag mRNAs stemming from the same cell (ProBac-seq[13], PETRI-seq[14], BacDrop[15], M3-seq[16], microSPLiT[7]). These latter approaches have made high-throughput single-cell RNA sequencing possible for a large number of prokaryotic cells. Here, we successfully applied the microSPLiT (microbial split-pool ligation transcriptomics)[7] approach to assess how a conjugative broad-host range plasmid influenced the subpopulation dynamics of *Pseudomonas putida*.

Plasmids are extrachromosomal semiautonomous mobile genetic elements (MGEs) that interact with their host genome to varying degrees. Plasmids use other host factors[17] such as nucleotides, tRNAs, amino acids, ribosomes, etc.[18] and thus participate in intracellular competition for resources[2]. More crude interactions also transpire, facilitated via plasmid-encoded regulatory elements[9,19], toxin-antitoxin systems[20] or other defense/antidefense systems[21]. The association of plasmids with a host can change its transcriptomic profile in a plasmid-host specific manner at the population level[22–24]. Plasmids can, for example, induce the use of alternative carbon sources or alter the metabolism of carbohydrates[23], amino acids and nucleotides[18] or respiration activities[23] and regulatory pathways[23,24]. The activation of an SOS response may also induce MGE interactions with potential deleterious effects for the host[18]. Over evolutionary time, compensatory mutations may reduce these genetic conflicts[18,25]. The above illustrates that plasmids interact with host chromosomes; however, very little is known about such interactions at the single-cell level and how these interactions may affect the subpopulation dynamics of their host.

Here, we sought to investigate transcriptional interactions between a conjugative broad-host-range plasmid and the host genome at the single-cell level. We compared bulk and single-cell transcriptomes and observed clear differences at the individual-cell level leading to the formation of subpopulations. We found that the *P. putida* population was heterogeneous and that the acquisition of a broad-host-range plasmid, which inflicted a population-wide burden, changed the subpopulation dynamics. Our data demonstrate that transcription of plasmid-encoded genes is highly variable at the single-cell level, suggesting a central role of heterogeneity in the evolutionary success of plasmids.

Results

Despite a small effect of plasmid carriage on growth, transcription of chromosomal genes is generally unaffected at the population level

Comparing the growth of *P. putida* growing separately with and without the broad-host-range plasmid pKJK5 showed a low but significant decrease in growth rate when carrying the plasmid at the start of the exponential phase (AUC 23.5±0.3 vs. 24.9±0,4, p=1.8×10^{-9}) (Fig. 1, Tab. S1). However, toward the end of the growth phase, no difference was observed. When growing plasmid-free and plasmid-carrier cells in coculture, in a competition experiment, the plasmid showed no significant fitness cost or advantage (w=1,016∓0,009) after 16 hours of cocultivation (Tab. S2). Plasmid impact on *P. putida* was explored by performing both population (bulk RNA-seq) and single-cell transcriptomics (microSPLiT) either carrying, or not, a conjugative incP-1 plasmid from independent cultures grown to OD0.5 and 1.5. Unsupervised cluster analyses of the population-level (bulk) gene transcripts (excluding tRNA and rRNA) separated samples according to growth state (OD0.5 vs. 1.5) and the presence/absence of the plasmid (Fig. S2). This separation, however, was mainly attributed to plasmid-encoded gene transcripts since after excluding these, the separation between plasmid-free and carrier populations was no longer supported statistically, despite differential transcription of a few chromosome-encoded genes (Fig. 1B&C).

microSPLiT generates quality scRNA-seq data apt for studying plasmid biology

Few studies have utilized the novel microSPLiT approach. Therefore, the acquired data were assessed by comparison to (i) population-level bulk transcriptomes (RNA-seq) and (ii) a blind microSPLiT replicate (referred to as the microSPLiT control) (Fig. S3). In contrast to the main microSPLiT experiment, the blind microSPLiT control was generated by mixing samples (plasmid presence/absence and growth state) before generating the microSPLiT libraries. The sum of mRNA transcripts per gene in the microSPLiT samples correlated well with those both from population-level (bulk) transcriptomes obtained from total mRNA extractions (r=0.793) and the microSPLiT control (r=0.944), showing that the single-cell data reflected population-level transcription. Importantly, this also indicates that microSPLIT did not introduce a systematic bias for specific transcripts. A total of 1599 single-cell transcriptomes were recovered, characterized by transcripts from 4432 different genes after discarding cells with less than 85 transcripts (Fig. S4C). On average, each contained 421.6 chromosomal transcripts. Among plasmid carrier cells, 91,4% displayed at least 1 plasmid transcript at OD0.5 and 94.8% at OD1.5, suggesting that the plasmid is stably maintained in *P. putida,* as shown in previous studies[26,27]. When performing microSPLiT, a trade-off between cell number and cell mRNA coverage exists. The microSPLiT control generated 3165 single-cell transcriptomes characterized by transcripts from 4248 genes with an average of 181.6 mRNA transcripts per cell (Fig. S4A&B).

Single-cell transcriptomics shows the formation of distinct subpopulations constrained by plasmid carriage

Unsupervised cluster analyses based on whole single-cell transcriptomes (plasmid- and chromosome-encoded transcripts) generated 9 distinct clusters using Euclidean distance-based K-nearest neighbor and Jaccard similarity projected on a uniform manifold approximation and projection (UMAP) plot (Fig. 2A). Clusters segregated according to growth state and plasmid carriage (Fig. 2A&B, S5). Cell transcriptomes from samples grown to OD0.5 were mainly distributed in clusters W1, W2, W8 and W9, while cells from OD1.5 were distributed in clusters W3-W7. At the outset of growth (OD0.5), clusters W1 and W9 were defined by plasmid-free cells, cluster W8 by plasmid-carrier cells, and cluster W2 contained

both plasmid-free and carrier cells (Fig. 2C). At OD1.5, clusters W3 and W4 were defined by plasmid-free cells, and clusters W5-W7 by plasmid-carrier cells.

In both population-level (Fig. S6) and single-cell transcriptomes (Fig. 2D), OD0.5 was characterized by a high number of transcripts from housekeeping genes such as ribosomal proteins (*rps*, *rpl*, *rpm, yce*D (PP_1910)), elongation factors (*efp*), protein translocators (*sec*E), RNAPs, global regulators (*rpo*BCD, *fur, fnrA, norR)*, and malate:quinone oxidoreductase (mqo-II). Induced transcription of these genes is typical for early exponential growth[28] and Mqo-II, for example, is regulated by carbon sources and oxygen availability, which change over time due to consumption[29]. At the end of the exponential phase (OD1.5), a high number of transcripts related to respiration in decreasing oxygen conditions characterized the samples. These included *cco*NOPQ-I, the outer membrane copper receptor *opr*C, the ubiquinol-cytochrome c reductase iron-sulfur subunit (*pet*A), the electron transfer flavoprotein subunit *etf*B, the porins *opr*D and *opr*Q, dipeptide transporters (*opd*P, *dpp*A-I), amino acid metabolisms (*put*AP, *ilv*CH, *arc*ABCD-1, *gdh*B), citrate synthase (*glt*A) and flagellin (*fli*C). A few genes discriminated plasmid-free and carrier cells, such as those encoding the septum site-determining protein *min*D, which covers the intracellular surface of the membrane during cell division to set the central position of the polar Z ring septum, the LPS-assembly protein (*lpt*D), the trigger factor (*tig*, chaperone), the mannose dehydratase (*gmd*) or amino acid transporters (*his*P, *put*P), whose abundance increases in the presence of pKJK5. Most of these genes also distinguished clusters obtained with cells from the control microSPLiT experiment (Fig. S7). Increased amounts of *lptD* and *minD* transcripts should lead to enlarged cells when the growth rate is lower, i.e., at the outset of growth. This indeed seemed to be the case, as flow cytometry analysis showed a small change in size and cell texture (Fig. S1). Increased cell size might have consequences for plasmid copy number, as plasmid replication was shown to be regulated by a size control mechanism[30]. However, these few differentially transcribed chromosome-encoded genes were not enough to discriminate plasmid-free and carrier cells at the whole transcriptome level.

Interestingly, looking at single-cell transcriptomics only, clusters W1, W4, W6 and W8 were distinct from clusters W2, W3, W5, W7 and W9 (Fig. 2A & 2D). The underlier of this separation did not seem to be related to growth state or plasmid presence/absence. Subpopulations W1, W4, W6 and W8 were characterized by increased levels of ribosomal proteins (*rpl* and *rps*), glutamine-like amino acid metabolism (*gln*A, *put*A) transcripts, the use of glycerol/glucose (*glp*K, *gln*K, *gap*A), chaperone transcripts (*grp*E, *hsl*O) and proteases (*prl*C, *prc*). This indicates that subpopulations with distinct transcriptomes co-occurred regardless of growth state, likely prompted through epigenetic determination.

Plasmid-encoded genes are differentially transcribed among cells, and a divergent subpopulation did not transcribe genes critical for conjugation

In addition to growth state, additional factors drive subpopulation dynamics. Cells highly transcribing plasmid-encoded genes belonged to clusters W8 (OD0.5) and W6 (OD1.5), which concomitantly displayed more ribosomal protein transcripts (*rps* and *rpl* genes; Fig. 2D) and more transcripts involved in glycerol (*glpK*, *gapA*) and glutamate metabolism (*glnA*, *glnK*, *putA*), proteases and stress proteins (*hslO*, *grpE*, *prc*).

To further investigate plasmid-gene transcription at the single-cell level, an unsupervised cluster analysis was performed including only plasmid transcripts from plasmid-carrier cells. These were normalized by dividing transcript counts by the summed plasmid-transcript number and performing log+1 transformation. A total of 6 plasmid transcriptome clusters were identified that grouped cells independently of growth state (Fig. 3A&S8). Cluster P1 mainly included cells from the whole genome clusters W5, W6 and W8. Clusters P3 and P4 contained more cells from cluster W2 and fewer cells from

W8 (Fig. 3B&C). Cells from cluster P1 displayed a high number of transcripts encoding proteins involved in mating pair formation (*trb* genes), *tra*C DNA primase, and different transposon-encoded genes (*tet*R, Tn402 and ISPa17 recombinase pKJK5-27). Cells from cluster P2 highly transcribed the DNA relaxase *tra*I, known to initiate oriT site-specific cleavage for replication, the ISPa17 insertion sequence, and the integrase *int*I1 from the Tn402-like transposon. Cells from cluster P3 highly transcribed the DNA primase *tra*C, cells from cluster P5 transcribed more trbG and trbL, a topoisomerase involved in mating pair formation, and cells from cluster P6 highly transcribed the *tra*L topoisomerase for the replication of pKJK5 during transfer **(Fig. 3D-E)**. Interestingly, the *tra*2 operon (*trb* genes encode the conjugative pilus, **Fig. 3F**) in our dataset was homogeneously expressed among plasmid carriers, but the transcriptional repressor *trb*A was present in a small number of cells that also had fewer transcripts of other genes of the *trb* operons **(Fig. 3E)**. The *kle*AB *and kle*EF genes, ensuring stable inheritance of the plasmid, were transcribed in a small number of cells from clusters P5 and P1, respectively, suggesting that these cells were about to divide **(Fig. 3D-E)**.

The *tra*GFEDC operon (Fig. 3F), which encodes genes involved in DNA replication and transfer and is essential for conjugation, stood out. As seen in Fig. 4A&B, the P4 plasmid cluster is notable, as genes of the *tra*GFEDC operon were not transcribed only in this subpopulation, which represented 12% of plasmid carriers. To confirm the occurrence of this subpopulation, the P_{traG} promoter of the *tra*GFEDC operon was fused with fluorescent protein sfGFP (P_{traG}-*sfGFP*) on the pPROBE-NT vector[31] to enable quantification of single-cell expression levels by flow cytometry. This validated that two subpopulations of cells co-occurred (Fig. 4C): one where P_{traG} was active (average 87%) and a smaller subpopulation with no P_{traG} activity (average 13%) at both ODs. Nonetheless, the P4 subpopulation did not seem to be inactive or consist of dead cells, as the numbers of *rps* and *rpl* ribosomal protein transcripts were equivalent to those of other plasmid-carrier cells (Fig. S9). Additionally, both microSPLiT and P_{traG}-*sfGFP* flow cytometry data showed that transcription of the *tra*GFEDC operon was higher at OD1.5 than at OD0.5 (Fig. 4B & C).

Plasmid carriage affects the transcription of host chromosomal genes, reducing subpopulation diversity

Chromosome-only single-cell transcriptomes formed 7 clusters (Ch1-7 clusters; Fig. 5A) showing transcriptional subpopulations with distinct chromosomal transcription profiles. At the beginning of the exponential phase (OD0.5), plasmid-free cells were evenly distributed among subpopulations Ch1, Ch3 and Ch7, while plasmid carriers were restricted to subpopulations Ch1 and Ch3, despite an equivalent number of captured transcripts/cell between plasmid-free and carrier cells (Tab. S3). At the end of the exponential phase (OD1.5), plasmid-free and carrier cells were equally distributed in the subpopulations (Ch2, Ch4, Ch5 and Ch6) but were spatially segregated on the UMAP projection (Fig. 4A-C), revealing a dissimilarity between chromosomal transcriptomes of plasmid-free and carrier cells. The subpopulations Ch5 and Ch6 were enriched in plasmid-carrier cells (Fig. 5C). When mapping chromosomal transcriptomes of plasmid-carriers (Fig. S10A-C) and plasmid-free cells (Fig. S10D-F) separately, cluster demarcation did not superimpose to the same degree, indicating that the presence of a plasmid contributed to changes in population heterogeneity. At OD0.5, cells were mainly distributed in 3 subpopulations. Interestingly, one of them (Ch7) did not contain plasmid-carrier cells (Fig. 5). Like other cells at the outset of growth (OD0.5), the Ch7 subpopulation transcribed genes involved in DNA conformation (*gyr*B), mRNA degradation (*pnp*), protein elongation (*efp*), succinyl-CoA synthetase (*suc*CD), glycolysis (*zwf*A), glycerol metabolism (glpD), fatty acid synthesis (PP_0368, *fad*B), or glutamate synthesis (*ybg*L). The Ch7 subpopulation, like most other OD0.5 cells, transcribed less glyceraldehyde-3-phosphate dehydrogenase (*gap*B), citrate synthase (*glt*A), import genes (*dpp*A-I, *opd*P, *opr*C, *opr*Q, *put*P) and branched-chain amino acid synthesis (*ilv*CHI). However, Ch7 cells were

characterized by transcripts that also defined cells at OD1.5. Indeed, when mapping Ch7 transcriptomes with the transcriptomes from the microSPLiT control, we see that those cells cluster with cells with OD1.5 transcripts (Fig. S12&S13). Increased transcription of genes involved in (i) respiration (use of *cco*NOP-I), (ii) arginine/lysine import (*arg*T), (iii) lysine oxidative decarboxylation (*dav*B), (iv) motility (fliC), and (v) the oxidative deamination of D-amino acids (*dad*A-II) was observed. Additionally, (vi) the production of ATP and N sources seemed to have shifted for anoxic arginine metabolism (increased number of transcripts for *arc*ABCD, *kau*B, *arg*E and decreased transcription of *car*BA, *arg*H and *arg*F) (Fig. 5D&E). Moreover, (vii) subpopulation Ch7 displayed reduced transcription of genes related to RNAP and global regulators, ribosomes, protein synthesis and translocation (*rpl* and *rps* genes, *rpo*ABCD, *rne*, *frr*, *asp*S, *pro*S, *tuf*A, *fus*A, *sec*E) and a higher number of transcripts related to protein catalysis (*prc*, *fts*H). (vii) Cells of subpopulation Ch7 also showed higher transcription of stress-related genes (PP_2187, PP_2648) and genes involved in pyruvate metabolism (*pyk*A, *edd*, *eda*). The chromosome single-cell transcriptome data suggest that cells in the Ch7 subpopulation used malate as a source for pyruvate synthesis (*mae*B), decreasing its use in the TCA cycle (decrease in *mqo*-II transcripts), and succinate formation was likely increased (*idh*, *suc*B) (Fig. 5, S11). Collectively, the differential expression patterns of cells in cluster Ch7 suggest that this subpopulation made a shift toward transcriptional patterns resembling later exponential growth despite the populations as a whole being in early exponential growth. Among the plasmid carriers at OD0.5, such a subpopulation did not arise.

Discussion

Here, we investigated transcription at the single-cell level of *P. putida* KT2440 with the conjugative broad-host-range IncP-1 plasmid pKJK5. *P. putida* KT2440 is widely used as a model bacterium in studies of soil bacteria and is important for biotechnology[32]. *P. putida* KT2440 has also been considered for bioremediation (e.g., [33]) and repeatedly used in studies of plasmid transfer in natural (e.g., [34-37]) and synthetic communities[38,39].

With microSPLiT, we observed that *P. putida*, despite growing in a continuously homogenized environment, displayed transcriptional heterogeneity. This is in agreement with the few other studies using similar approaches[7,14,15] on bacteria from different orders. Cells clustered into transcriptional subpopulations, displaying differential expression of ribosomal proteins and alternative amino acid and carbon metabolisms. These subpopulations may arise due to microenvironmental differences, epigenetic determination, phase variation[2] and/or mutations[40]. Considering our experimental setup, it is unlikely that the transcriptional subpopulations identified were generated by arising mutations, as the cells only grew for a few generations and the mutation rate of *P. putida* is relatively low. Bacteria were grown with constant shaking in large bottles, making it unlikely that microenvironmental differences arose to a degree that could explain the observed subpopulations. Instead, these subpopulations likely manifest to optimize the population-wide fitness of the genotype by facilitating bet-hedging or division of labor strategies.

The subpopulation Ch7 of plasmid-free cells collected at OD0.5 seems to undergo a diauxic shift and/or co-utilization of carbon sources[41,] which have been shown to occur through stochastic events in isogenic populations[42]. The of carbon sources by plasmid-free cells may have led to differences in growth rates observed between plasmid-free and carrier cells since, during early exponential growth, no plasmid carriers adopted the transcriptome profile of subpopulation Ch7. The stability of pKJK5 within a bacterial population is ensured by efficient conjugation[43], genes ensuring stable inheritance (partitioning system *par*A and *inc*C; *klc* and *kle* genes[43]), and a replication system that enlarges the host range of the plasmid, especially among proteobacteria[44]. However, its stability in a subpopulation of cells seems to also depend

on the transcriptomic context. This shift, combined with the cost of plasmid carriage, may have induced a low energy status of the host cells, suggesting that the plasmid compromised the potential of the *P. putida* population to generate subpopulations, impeding them from meeting the burden of plasmid maintenance[45]. The Ch7 subpopulation was characterized by a higher number of transcripts involved in arginine metabolism and the expulsion of ornithine. The plasmid may thus have deprived the population of plasmid carriers of an alternative ATP/NH_3^+ source in addition to extracellular ornithine, which was shown to act as a public good for *Streptococcus* species[46,47].

Clustering of cells based on plasmid-encoded transcripts correlated with the transcriptional activity of ribosomes and amino acid and carbon metabolisms. When investigating heterogeneity in transcription among plasmid-encoded genes, we observed that the *trb*A repressor was transcribed heterogeneously in the population, which would have direct consequences for the transcription of the rest of the operon. Genes encoding the topoisomerases *tra*L and *trb*L and the *kle* genes, ensuring stable inheritance of the plasmid, were transcribed in distinct subpopulations of cells. The low copy number of these transcripts might make their detection harder. Nevertheless, it highlights heterogeneity in their transcription, suggesting that these stability factors only need to be transcribed differentially despite their importance for plasmid maintenance and should be investigated further. Likewise, we show that the transcription of transposases and integrases associated with transposons encoded by pKJK5 was also limited to a specific subset of cells. Similar observations were made in another single-cell transcriptome study[48] and we speculate that these MGEs, in part, rely on stochastic induction of transposition, as observed with stochastic lysis by bacteriophages[49]. This could represent a bet-hedging-like strategy, as transposition events can have large implications on host fitness and the success of the transposon itself. Last, we show with both microSPLiT and a P_{trbG}-*sfGFP* activity reporter that a defined subpopulation of cells did not transcribe the *tra*GFEDC operon and thus does not engage in conjugation. It may seem counterintuitive that the plasmid does not maximize its potential for horizontal transfer; however, decreasing the expression of the large conjugative machinery is likely to decrease its burden at the level of the overall population.

This study is among the first to discern the role of bacterial subpopulations in plasmid biology. Using microSPLiT, we illustrate that transcriptional heterogeneity among cells is indeed central to the biology of plasmids. Plasmid carriage impacted the subpopulation dynamics of the host, and the transcription of plasmid-encoded genes was highly heterogeneous. Central plasmid functions such as replication and maintenance seem to fluctuate, likely in sync with the cell cycle, while transcription of genes critical for conjugation was biphasic, resulting in a smaller subpopulation that likely does not engage in conjugation. Beginning to understand subpopulation dynamics holds great promise for the understanding of bacterial ecology and evolution and for biotechnological applications. An important perspective of the findings presented here is that we need to further understand single-cell heterogeneity in plasmid biology at a broader scale and in natural environments where microbes experience a large diversity of environmental factors. A better understanding of plasmids and other MGEs (e.g., [50]) will be critical to constrain the ongoing antibiotic resistance crisis.

Methods

Bacterial strains, cultures, growth curve, and competition experiment

Pseudomonas putida KT2440 growth was performed on Lysogeny-Broth medium (LB) at 30°C and 250 RPM. *Pseudomonas putida* KT2440/pKJK5 was obtained by electroporating 1 µg of pKJK5 plasmid into 50 µL of competent *P. putida* KT2440. Competency was achieved at an optical density (600 nm) of 0.8.

A culture of 50 mL was washed twice with 50 mL of 10% ice-cold glycerol and finally resuspended in 800 µL of 10% ice-cold glycerol. Cells were aliquoted (50 µL) and electroporated in a 2 mm cuvette at a voltage of 2,400 V, 1 pulse. For the following experiments, *P. putida* KT2440 and *P. putida* KT2440/pKJK5 were precultured separately overnight in 5 mL of LB medium. *Pseudomonas putida* KT2440/pKJK5 was cultivated with tetracycline (50 µg/mL). For the growth curves (3 biological replicates, 4 technical replicates), precultures were washed in LB medium and diluted 10^4 times before distributing 200 µL in a 96-well plate incubated at 30°C and shaken every 20 minutes. Optical density (600 nm) was recorded after shaking using a Synergy H1 microplate reader (BioTek, Winooski, VT). For the competition experiment (4 biological replicates), overnight cultures were washed in LB medium and mixed (*Pseudomonas putida* KT2440 + *Pseudomonas putida* KT2440/pKJK5) equally. The mixes were diluted 10^4 times, and 800 µL was distributed in a 12-well plate. Total cell number and plasmid carriers were counted before and after competition using a 10^5-fold dilution plated on LB plates and LB and tetracycline 20 µg/mL, respectively. The fitness of the plasmid was calculated as $w=\ln(P_{carrier_f}/P_{carrier_i})/\ln(P_{free_f}/P_{free_i})$. For the transcriptomics analyses, 100 mL cultures were incubated in flasks from a 200-fold dilution and sampled at 600 nm optical densities of 0.5 and 1.5.

GFP-based reporter plasmid and flow cytometry analysis

The promoter *Ptra*G was cloned using HiFi Gibson Assembly into a pPROBE-NT backbone with primers traGp_Fw (5'-gttagttagggaataagccgagttttaagggagcctcgcgg-3') and traGp_Rv (5'-aggtcgactctagaggatcggccaggaagagggctaaag-3') to amplify the P_{traG} region from pKJK5 with overhangs to pPROBE-NT and primers MFHO38 (5'-gatcctctagagtcgacctgc-3) and MFHO37 (5'-tcggcttattccctaactaactaaag-3') for pPROBE-NT. The GFP reporter plasmids were transformed into *P. putida* KT2440 (negative control) and *P. putida* KT2440/pKJK5 following the electroporation procedure. Overnight cultures were diluted 1/50 and normalized to an OD of 0.1. These cultures (n=3) were then grown at 30°C and 250 RPM. For cell size and granulometry, samples were taken at OD0.5 and 1.5 and examined by flow cytometry (FACS Aria III, Becton Dickinson Biosciences, San Jose, CA, USA) using the 488 nm laser and the FSC and SSC detection channels, respectively. To measure GFP intensity and abundance, samples were taken at OD0.5 and OD1.5, washed twice with PBS and examined by flow cytometry using a 488 nm excitation laser and the FITC (530/30 nm bandpass filter) detector channel. The closing gate was set at 50,000 counts using the FSC and SSC detection channels. A culture of *P. putida* KT2440/pKJK5 containing the pPROBE-NT plasmid was used as a control to set up the gate for the GFP signal on the FITC detection channel. The data in Fig. 4 were analyzed using FlowJo software (Tree Star Inc., USA).

Transcriptomic data acquisition

After an overnight culture of 16 hours in 5 mL of selective LB (250 RPM), *Pseudomonas putida* KT2440 and *Pseudomonas putida* KT2440/pKJK5 were washed and diluted 500 times in 100 mL of LB. Flasks were incubated at 30°C (250 RPM), and cultures were sampled at turbidities (600 nm) of 0.5 and 1.5.

Population-level (bulk) RNA-seq

Samples (N=4) were centrifuged (3 minutes, 7000xg), RNA content was directly extracted using the Quick-RNA Fungal/Bacterial Miniprep Kit (Zymo Research, CA, USA) following the manufacturer's instructions, and libraries were prepared using the Zymo-Seq RiboFree Total RNA Library Kit (Zymo Research, CA, USA). Fragment integrity and size were assessed using a fragment analyzer (Agilent, CA, USA) and quantified with a Qubit dsDNA HS assay kit (Thermo Fisher Scientific, Waltham, MA, USA)

before sequencing on a Novaseq 6000 (Illumina, CA, USA) at 2 ×150 bp performed by Novogene Co., Ltd. (Cambridge, United Kingdom). Sequence files can be found at NCBI under Bioproject ID PRJNA1019643.

microSPLiT scRNA-seq

The experiment was repeated 2 times. Samples were centrifuged (3 minutes, 7000xg), resuspended in the same volume of cold paraformaldehyde 4% (pH 7.2) for fixation and kept in a refrigerator overnight. In-cell mRNA tagging, lysis and library preparation were performed as described previously[7].

Briefly, fixed samples were permeabilized by lysozyme, and a polyA queue was added to mRNA using *E. coli* Poly(A) Polymerase (New England Biolabs, Ipswich, MA). Cell subsamples were stained with SYBR™ Green I (Thermo Fisher Scientific, Waltham, MA, USA), and their concentration in each sample was measured using a FACS Aria III (Becton Dickinson Biosciences, San Jose, CA, USA). A total of 250,000 cells were distributed in 48 wells where reverse transcription occurred (Maxima H Minus Reverse Transcriptase, Thermo Scientific™, Thermo Fisher Scientific, Villebon sur Yvette. France), each well containing primers with a specific barcode. Cell distribution was carried out blindly during the first experiment, while P-0.5, P-1.5, P+0.5 and P+1.5 samples were knowingly distributed among the 48 wells. After reverse transcription, the cells were pooled together and physically separated (vortex and filtration steps at 10 and 1 µm, pluriSelect Life Science UG (haftungsb.) & Co. KG, Leipzig, Germany) and randomly split into 96 wells where a well-specific oligo was added to the cDNA construct by ligation with a T4 DNA Ligase (New England Biolabs, Ipswich, MA). Cell pooling, random splitting and ligation were repeated for a third barcode addition so that, statistically, cell-hosted cDNAs carry a unique 3-barcode combination. Cells were pooled, divided into sublibraries of 10 000 (replicate 1) or 6 000 cells (replicate 2) and lysed after measuring their concentration using a FACS Aria III (Becton Dickinson Biosciences, San Jose, CA, USA). The second strand synthesis was performed using template switching oligos, and cDNAs were amplified using a KAPA HiFi HotStart ReadyMix PCR kit (Roche Sequencing Solutions, Pleasanton, CA) supplemented with EvaGreen® Dye (Biotium, San Francisco, CA) for 14 cycles in total. Sublibraries were fragmented using Enzymatics Fragmentase (QIAGEN Beverly, Beverly, CA) and amplified. Sublibrary-specific adapters were ligated using Enzymatics ligase (QIAGEN Beverly, Beverly, CA), and sublibraries of cDNA were amplified using a KAPA HiFi HotStart ReadyMix PCR kit (Roche Sequencing Solutions, Pleasanton, CA).

Fragment integrity and size were assessed using a Fragment Analyzer (Agilent, CA, USA) using an NGS Fragment Kit (1-6000 bp) and quantified with a Qubit dsDNA HS assay kit (Thermo Fisher Scientific, Waltham, MA, USA) before sequencing on a Novaseq 6000 (Illumina, CA, USA) at 2×150 bp performed by Novogene Co., Ltd. (Cambridge, United Kingdom). A list of primers and associated barcodes can be found in Kuchina et al, 2021[7]. Sequence files can be found at NCBI under Bioproject ID: PRJNA1019643. The number of cells and transcripts per cell were equivalent in the different generated sublibraries (Fig. S4B).

Computational method

The reference genome was generated using STAR (https://github.com/alexdobin/STAR) combining the pKJK5 plasmid GenBank record AM261282.1 and *Pseudomonas putida* KT2440 genome (ASM756v2 on EnsemblBacteria). The reference genome was indexed for STAR using parameters (--genomeSAindexNbases 10) specific for small genomes using the formula min(14, log2 (Genome Length)/2 - 1). The created genome was used as a reference for both approaches (bulk & microSPLiT).

Population-level (bulk) RNA-seq

The sequenced reads were trimmed of the remaining adapter sequences and low quality based using bbduk (BBMap–Bushnell B. – sourceforge.net/projects/bbmap/), with right-side trimming using parameters {k=23 mink=11 hdist=1 tpe tbo trimq=10}. Trimmed reads were mapped against the reference genome, and the per-cell gene counts were quantified using STAR (https://github.com/alexdobin/STAR). Transcripts identified as rRNA, tRNA and plasmid encoded were removed from the data. Feature counts from the generated contingency table (gene x sample) were center-scaled and normalized (divided by the total counts, multiplied by 10 000+1, and log10 transformed).

microSPLiT scRNA-seq

Sequenced reads were demultiplexed (barcode list can be found in Supplemental Data) and mapped against the reference genome, and the per-cell gene expression was quantified using STARsolo (https://github.com/alexdobin/STAR/). A matrix of unique molecular identifier (UMIs, unique gene transcript-associated barcode) counts for each cell (N-by-K matrix, with N cells and K genes) was generated by gathering cells from all sublibraries. UMIs identified as rRNA or tRNA were removed from the dataset, and cells with less than 100 UMIs were sorted out. UMIs identified as plasmid genes were counted and added as metadata to characterize cells, as well as the sublibrary, the associated experiment and the sample type. Data were subset as follows: subset A contains chromosome-encoded UMIs of all cells; subset B contains chromosome-encoded UMIs of plasmid-carrier cells; subset C contains chromosome-encoded UMIs of plasmid-free cells; and subset D contains plasmid-encoded UMIs of all cells. For each subset of data, a SeuratObject was created using the R package Seurat 4.2.1., retaining features present in at least 3 cells. Feature counts per cell were divided by the total counts of the cell, log10 normalized and scaled. Linear dimensional reduction was performed with a PCA, and dimensionality was selected by combining a JackStraw resampling test and an elbow plot. Cells were clustered with an integrative approach combining a KNN graph based on the Euclidean distance, refining the edge weights with Jaccard similarity and the Louvain algorithm. A nonlinear dimensional reduction was then applied with UMAP (https://github.com/lmcinnes/umap).

Data availability

All sequence data produced in this publication are publicly available through the National Center for Biotechnology Information's SRA repository under accession number PRJNA1019643.

Acknowledgments

This work was supported by Villum Fonden (BioRep-HGT, Grant No. 00028304) and by the Fond National de Recherche Scientifique (FNRS-F.R.S). We acknowledge the use of computing resources at the core facility for biocomputing at the Department of Biology, University of Copenhagen. We would like to thank Prof. Lars Hestbjerg Hansen and Assistant Prof. Witold Piotr Kot for help in sequencing to verify the quality of the initial microSPLiT-seq libraries.

Author contributions

V.C. and J.S.-M. conceived the study and designed the laboratory experiments. V.C and R.I.-C. carried out the laboratory experiments and conducted the analysis of the experimental data. J.S.-M. and J.N contributed to materials and analysis tools. A.K. and G.S. provided protocols and expertise. All authors discussed the theory and wrote the manuscript.

Competing interests

The authors declare no competing interests.

Additional information

Supplementary tables and figures can be found in the supplementary information document.

References

1. Han, Y. & Zhang, F. Heterogeneity coordinates bacterial multi-gene expression in single cells. *PLoS Comput. Biol.* 16, 1–17 (2020).

2. van Vliet, S., et al. Spatially Correlated Gene Expression in Bacterial Groups: The Role of Lineage History, Spatial Gradients, and Cell-Cell Interactions. *Cell Syst.* 6, 496-507.e6 (2018).

3. Rosenthal, A. Z. et al. Metabolic interactions between dynamic bacterial subpopulations. *Elife* 7, 1–18 (2018).

4. Grimbergen, A. J., Siebring, J., Solopova, A. & Kuipers, O. P. Microbial bet-hedging: The power of being different. *Curr. Opin. Microbiol.* 25, 67–72 (2015).

5. Lim, Han N., and Alexander Van Oudenaarden. "A multistep epigenetic switch enables the stable inheritance of DNA methylation states." Nature genetics 39(2), 269-275 (2007).

6. Christen, M., Kulasekara, H. D., Christen, B., Kulasekara, B. R., Hoffman, L. R., & Miller, S. I. Asymmetrical distribution of the second messenger c-di-GMP upon bacterial cell division. Science, 328(5983), 1295-1297 (2010).

7. Kuchina, A. et al. Microbial single-cell RNA sequencing by split-pool barcoding. *Science (80-.).* 371, 1–9 (2021).

8. Dubnau, D. & Blokesch, M. Mechanisms of DNA Uptake by Naturally Competent Bacteria. *Annu. Rev. Genet.* 53, 217–237 (2019).

9. Vial, L., and Hommais, F. Plasmid-chromosome cross-talks. *Environ. Microbiol.* 22, 540–556 (2020).

10. Dar, D., Dar, N., Cai, L., and Newman, D. K. Spatial transcriptomics of planktonic and sessile bacterial populations at single-cell resolution. Science 373(6556), eabi4882 (2021).

11. Sheng, K., Cao, W., Niu, Y., Deng, Q., and Zong, C. Effective detection of variation in single-cell transcriptomes using MATQ-seq. Nat. Methods 14, 267–270 (2017).

12. Imdahl, F., Vafadarnejad, E., Homberger, C., Saliba, A., and Vogel, J. Single-cell RNA-sequencing reports growth-condition-specific global transcriptomes of individual bacteria. *Nat. Microbiol. Lett.* 5, 1202–1206 (2020).

13. McNulty, R., Sritharan, D., Pahng, S.H. et al. Probe-based bacterial single-cell RNA sequencing predicts toxin regulation. *Nat Microbiol* 8, 934–945 (2023).

14. Blattman, S. B., Jiang, W., Oikonomou, P., and Tavazoie, S. Prokaryotic single-cell RNA sequencing by in situ combinatorial indexing. *Nat. Microbiol.*5(10), 1192-1201 (2020).

15. Ma, P., Amemiya, H. M., He, L. L., Gandhi, S. J., Nicol, R., Bhattacharyya, R. P., et al. Bacterial droplet-based single-cell RNA-seq reveals antibiotic-associated heterogeneous cellular states. *Cell*, 1–15 (2023).

16. Gitai, Z., Wingreen, N. S., Adamson, B., Lin, A. E., Koch, M. D., Yuan, J., et al. Massively-parallel Microbial mRNA Sequencing (M3-Seq) reveals heterogeneous behaviors in bacteria at single-cell resolution. *bioRxiv*, 2022.09.21.508688 (2022).

17. San Millan, A. & MacLean, R. C. Fitness Costs of Plasmids: a Limit to Plasmid Transmission. *Microbiol. Spectr.* 5, 1–12 (2017).

18. Hall, J. P. J. et al. Plasmid fitness costs are caused by specific genetic conflicts enabling resolution by compensatory mutation. PLOS Biology 19(10): e3001225 (2021).

19. Thompson, C. M. A., Hall, J. P. J., Chandra, G., Martins, C., Saalbach, G., Bird, S., et al. (2023). Plasmid manipulation of bacterial behaviour through translational regulatory crosstalk. *PLoS Biol.* 21, e3001988 (2021).

20. Ni, Songwei, et al. "Conjugative plasmid-encoded toxin–antitoxin system PrpT/PrpA directly controls plasmid copy number." Proceedings of the National Academy of Sciences 118(4), e2011577118 (2021).

21. Wang, L., Xie, X., Lv, B., Liu, Y., Li, W., Zhang, Z., et al. A bacterial Argonaute with efficient DNA and RNA cleavage activity guided by small DNA and RNA. Cell Rep. 41, 111533 (2022).

22. San Millan, A. et al. Integrative analysis of fitness and metabolic effects of plasmids in *Pseudomonas aeruginosa* PAO1. *ISME J.* 12, 3014–3024 (2018).

23. Takahashi, Y. et al. Modulation of primary cell function of host Pseudomonas bacteria by the conjugative plasmid pCAR1. *Environ. Microbiol.* 17, 134–155 (2015).

24. San Millan, A., Toll-Riera, M., Qi, Q. & MacLean, R. C. Interactions between horizontally acquired genes create a fitness cost in *Pseudomonas aeruginosa*. *Nat. Commun.* 6, 1–8 (2015).

25. Kawano, H., Suzuki-Minakuchi, C., Sugiyama, D., Watanabe, N., Takahashi, Y., Okada, K., et al. A Novel Small RNA on the *Pseudomonas putida* KT2440 Chromosome Is Involved in the Fitness Cost Imposed by IncP-1 Plasmid RP4. Front. Microbiol. 11 (2020).

26. Bahl, M. I., Hansen, L. H., and Sørensen, S. J. Impact of conjugal transfer on the stability of IncP-1 plasmid pKJK5 in bacterial populations. FEMS Microbiol. Lett. 266, 250–256 (2007).

27. Røder, Henriette Lyng, et al. "Biofilms can act as plasmid reserves in the absence of plasmid specific selection." npj Biofilms and Microbiomes 7(1), 78 (2021)

28. Yuste, L., Hervás, A. B., Canosa, I., Tobes, R., Jiménez, J. I., Nogales, J., et al. Growth phase-dependent expression of the *Pseudomonas putida* KT2440 transcriptional machinery analysed with a genome-wide DNA microarray. *Environ. Microbiol.* 8, 165–177 (2006).

29. Van der Rest, M. E., Frank, C., and Molenaar, D. Functions of the membrane-associated and cytoplasmic malate dehydrogenases in the citric acid cycle of *Escherichia coli*. J. Bacteriol. 182, 6892–6899 (2000).

30. Keasling, J. D., Palsson, B. O., and Cooper, S. Cell-cycle-specific F plasmid replication: Regulation by cell size control of initiation. *J. Bacteriol.* 173, 2673–2680 (1991).

31. Miller WG, Leveau JH, Lindow SE. Improved gfp and inaZ broad-host-range promoter-probe vectors. Mol Plant Microbe Interact. Nov;13(11), 1243-50 (2000).

32. Ankenbauer, A., Schäfer, R. A., Viegas, S. C., Pobre, V., Voß, B., Arraiano, C. M., et al. *Pseudomonas putida* KT2440 is naturally endowed to withstand industrial-scale stress conditions. Microb. Biotechnol. 13, 1145–1161 (2020).

33. Gong, T., Liu, R., Che, Y., Xu, X., Zhao, F., Yu, H., et al. Engineering *Pseudomonas putida* KT2440 for simultaneous degradation of carbofuran and chlorpyrifos. Microb. Biotechnol. 9, 792–800 (2016).

34. Klümper, U., Riber, L., Dechesne, A., Sannazzarro, A., Hansen, L. H., Sørensen, S. J., et al. Broad host range plasmids can invade an unexpectedly diverse fraction of a soil bacterial community. ISME J. 9, 934–945 (2015).

35. Cyriaque, V., Jacquiod, S., Riber, L., Abu Al-soud, W., Gillan, D. C., Sørensen, S. J., et al. Selection and propagation of IncP conjugative plasmids following long-term anthropogenic metal pollution in river sediments. *J. Hazard. Mater.* 382, 121173 (2020).

36. Jacquiod, S., Brejnrod, A., Morberg, S. M., Abu Al-Soud, W., Sørensen, S. J., and Riber, L. Deciphering conjugative plasmid permissiveness in wastewater microbiomes. *Mol. Ecol.* 26, 3556–3571 (2017).

37. Fan, X. T., Li, H., Chen, Q. L., Zhang, Y. Sen, Ye, J., Zhu, Y. G., et al. Fate of antibiotic resistant pseudomonas putida and broad host range plasmid in natural soil microcosms. Front. Microbiol. 10, 194 (2019).

38. Hall, J. P. J., Wood, A. J., Harrison, E., and Brockhurst, M. A. Source–sink plasmid transfer dynamics maintain gene mobility in soil bacterial communities. Proc. Natl. Acad. Sci. 113, 8260–8265 (2016).

39. Cyriaque, V., Madsen, J. S., Fievez, L., Leroy, B., Hansen, L. H., Bureau, F., et al. Lead Drives Complex Dynamics of a Conjugative Plasmid in a Bacterial Community. Front. Microbiol. 12, 1–14 (2021).

40. Vincent, M. S., and Uphoff, S. Bacterial phenotypic heterogeneity in DNA repair and mutagenesis. Biochem. Soc. Trans. 48, 451–462 (2020).

41. Perrin, E., Ghini, V., Giovannini, M., Di Patti, F., Cardazzo, B., Carraro, L. et al. Diauxie and coutilization of carbon sources can coexist during bacterial growth in nutritionally complex environments. Nature communications, 11(1), 3135 (2020).

42. Solopova, A., Van Gestel, J., Weissing, F. J., Bachmann, H., Teusink, B., Kok, J., & Kuipers, O. P. Bet-hedging during bacterial diauxic shift. Proceedings of the National Academy of Sciences, 111(20), 7427-7432 (2014).

43. Bahl, M. I., Hansen, L. H., and Sørensen, S. J. Impact of conjugal transfer on the stability of IncP-1 plasmid pKJK5 in bacterial populations. *FEMS Microbiol. Lett.* 266, 250–256 (2007).

44. Li, L., Dechesne, A., Madsen, J. S., Nesme, J., Sørensen, S. J., and Smets, B. F. Plasmids persist in a microbial community by providing fitness benefit to multiple phylotypes. *ISME J.* 14, 1170–1181 (2020).

45. Rysz, M., Mansfield, W. R., Fortner, J. D., and Alvarez, P. J. J. Tetracycline Resistance Gene Maintenance under Varying Bacterial Growth Rate, Substrate and Oxygen Availability, and Tetracycline Concentration. *Environ. Sci. Technol.* 47, 6995–7001 (2013).

46. Fulde, M., Willenborg, J., Huber, C., Hitzmann, A., Willms, D., Seitz, M., et al. The arginine-ornithine antiporter arcD contributes to biological fitness of streptococcus suis. *Front. Cell. Infect. Microbiol.* 4, 1–10 (2014).

47. Sakanaka, A., Kuboniwa, M., Takeuchi, H., Hashino, E., and Amano, A. Arginine-ornithine antiporter ArcD controls arginine metabolism and interspecies biofilm development of Streptococcus gordonii. *J. Biol. Chem.* 290, 21185–21198 (2015).

48. Ma, P., Amemiya, HM., He LL., Gandhi, SJ., Nicol, R., Bhattacharyya, RP., Smillie CS., Hung DT. Bacterial droplet-based single-cell RNA-seq reveals antibiotic-associated heterogeneous cellular states. Cell. 2023 Feb 16;186(4), 877-891.e14 (2023).

49. Joh, RI., Weitz, JS. To lyse or not to lyse: transient-mediated stochastic fate determination in cells infected by bacteriophages. PLoS computational biology. 7(3), e1002006 (2011).

50. Ibarra-Chávez, R., Brady, A., Chen, J., Penadés, JR., Haag, AF. Phage-inducible chromosomal islands promote genetic variability by blocking phage reproduction and protecting transductants from phage lysis. PLOS Genetics 18(3), e1010146 (2022).

Figure legends

Fig. 1: Small growth effect of plasmid carriage with little influence on chromosomal gene transcription at the population level. (A) Growth curve (OD=600 nm) showing small differences in growth rates of *Pseudomonas putida* KT2440 with (blue) and without (red) pKJK5 (Kruskal–Wallisχ^2 =16.516; p= 4.823e-05) and area under the curve (t= 10.045; p=1.792e-09) (see Tab. S1). Samples were taken at OD0.5 and OD1.5 for bulk transcriptomics or microSPLiT sample preparation (indicated by colored circles). (B) PCA multivariate analysis on transcripts from chromosome-encoded genes at the population level (bulk) according to the presence (P+) or absence (P-) of the plasmid and according to ODs (0.5 vs. 1.5). The presence of the plasmid did not significantly discriminate between cell transcriptomes, as confirmed using 10,000 permutations in a PERmutational Multivariate ANalysis Of VAriance (PERMANOVA; $r^2_{plasmid}$=0.094; $p_{plasmid}$=0.0922; r^2_{OD}= 0.253; p_{OD}=0.001; $r^2_{plasmid: OD}$= 0.035; $p_{plasmid: OD}$=0.7).

Fig. 2. Whole single-cell transcriptomes generally cluster in accordance with growth state and the presence/absence of the plasmid. Subpopulation clustering identified by single-cell transcriptomics of *P. putida* carrying a plasmid (P+) or not (P-) at early (OD0.5) and late exponential growth (OD1.5). (A) UMAP obtained by microSPLiT scRNA sequencing identified 9 whole transcriptome clusters (W1-W9) where both plasmid and chromosomal transcripts were analyzed. The dashed line indicates cluster separation not linked to growth state or the presence/absence of plasmid. (B) Clusters segregate cell transcriptomes in subpopulations separating the two different growth states (OD0.5 and 1.5). (C) Cell transcriptomes from OD0.5 were mainly distributed in clusters W1, W2, W8 and W9, while cells from OD1.5 were mainly distributed in clusters W3-W7. (D) Heatmap of the normalized number of transcripts per cell. The top 10 biomarker genes identified by the Wilcoxon signed-rank test are shown for each cluster. (E) Heatmap obtained by averaging the normalized transcription of differentially expressed gene transcripts from the single-cell transcriptomes. Data from different growth states and the presence/absence of plasmids were grouped.

Fig. 3. Plasmid single-cell transcriptome clustering suggests population heterogeneity in plasmid gene transcription, independent of growth state. Subpopulation clustering identified by single-cell transcriptomics of *P. putida* carrying the plasmid at early (OD0.5) and late exponential growth (OD1.5). (A) UMAP obtained by microSPLiT scRNA sequencing identified 6 plasmid transcriptome clusters (P1-P6) when only plasmid transcripts were analyzed. (B) Dots representing single-cell plasmid transcriptomes overlaid with colors indicating whole transcriptome clusters (W1-9), as shown in Figure 2A. (C) Normalized distribution of whole-cell transcriptomes within the six different clusters found based on plasmid single-cell transcriptomes. (D) Heatmap of the normalized number of transcripts per cell ordered according to clusters P1-6. (E) Normalized transcript counts of selected genes from individual cells displayed on top of the UMAP generated with the plasmid single-cell transcriptomes. (F) Genome map of the pKJK5 plasmid made with SnapGene.

Fig. 4. Subpopulation transcriptional heterogeneity of the *traGFEDC* operon, which is essential for conjugation, validated by flow cytometry of the promoter-*sfGFP* fusion reporter. (A) Heatmap of the normalized number of *tra* gene transcripts per cell ordered according to clusters P1-6. (B) Normalized summed transcript counts of traGFEDC genes from individual cells displayed on top of the UMAP generated with the plasmid single-cell transcriptomes and on a violin plot according to OD. (C) Flow cytometry histogram for *PtraG-sfGFP* signal and GFP cell counts from samples taken at OD0.5 and OD1.5.

Fig. 5. Chromosome single-cell transcriptomes generally cluster in accordance with growth state, yet the subpopulation dynamics are influenced by plasmid carriage. Subpopulation clustering identified by single-cell transcriptomics of *Pseudomonas putida* carrying the plasmid (P+) or not (P-) at early (OD0.5) and late exponential growth (OD1.5). Only chromosomal gene transcripts were analyzed. (A) UMAP of transcriptomes of *P. putida* obtained with microSPLiT RNA sequencing, identifying 7 (Ch1-Ch7) clusters. (B) Clusters segregate cell transcriptomes in subpopulations separating the 2 different growth states (OD0.5 and 1.5). (C) Cell transcriptomes from OD0.5 were mainly distributed in clusters Ch1, Ch3 and Ch7, while cells from OD1.5 were mainly distributed in clusters Ch2, Ch4, Ch5 and Ch7. (D) Heatmap of biomarker genes of the different Ch clusters. An exhaustive

heatmap can be found in Fig S11. (E) Schematic representation of upregulated (green) or downregulated (red) genes in cells from cluster Ch7. Created with BioRender.com.

Figures

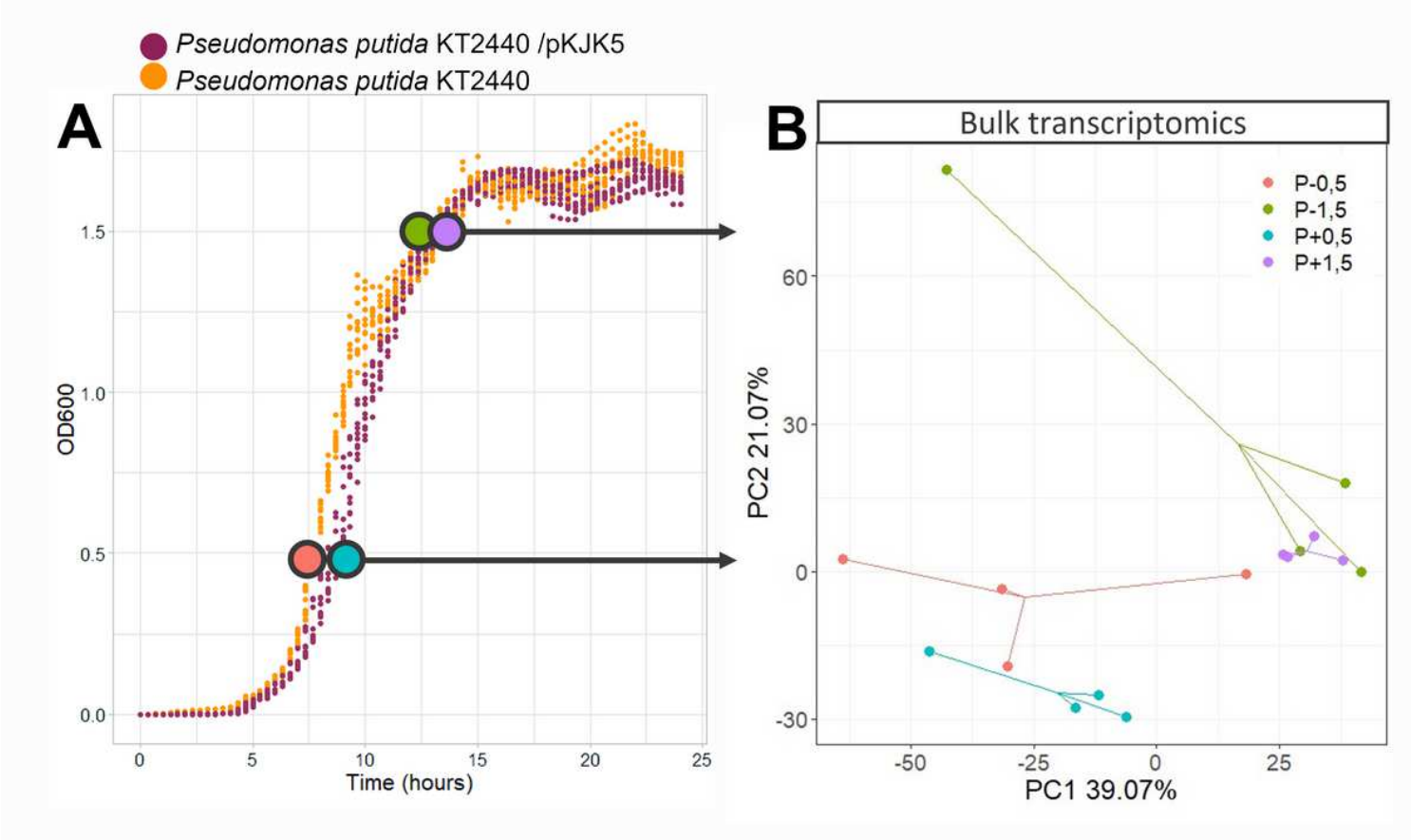

Figure 1

Small growth effect of plasmid carriage with little influence on chromosomal gene transcription at the population level. (A) Growth curve (OD=600 nm) showing small differences in growth rates of Pseudomonas putida KT2440 with (blue) and without (red) pKJK5 (Kruskal Wallisχ^2 =16.516; p= 4.823e-05) and area under the curve (t= 10.045; p=1.792e-09) (see Tab. S1). Samples were taken at OD0.5 and OD1.5 for bulk transcriptomics or microSPLiT sample preparation (indicated by colored circles). (B) PCA multivariate analysis on transcripts from chromosome-encoded genes at the population level (bulk) according to the presence (P+) or absence (P-) of the plasmid and according to ODs (0.5 vs. 1.5). The presence of the plasmid did not significantly discriminate between cell transcriptomes, as confirmed using 10,000 permutations in a PERmutational Multivariate ANalysis Of VAriance (PERMANOVA; r^2plasmid=0.094; pplasmid=0.0922; r^2OD= 0.253; pOD=0.001; r^2plasmid: OD= 0.035; pplasmid: OD=0.7).

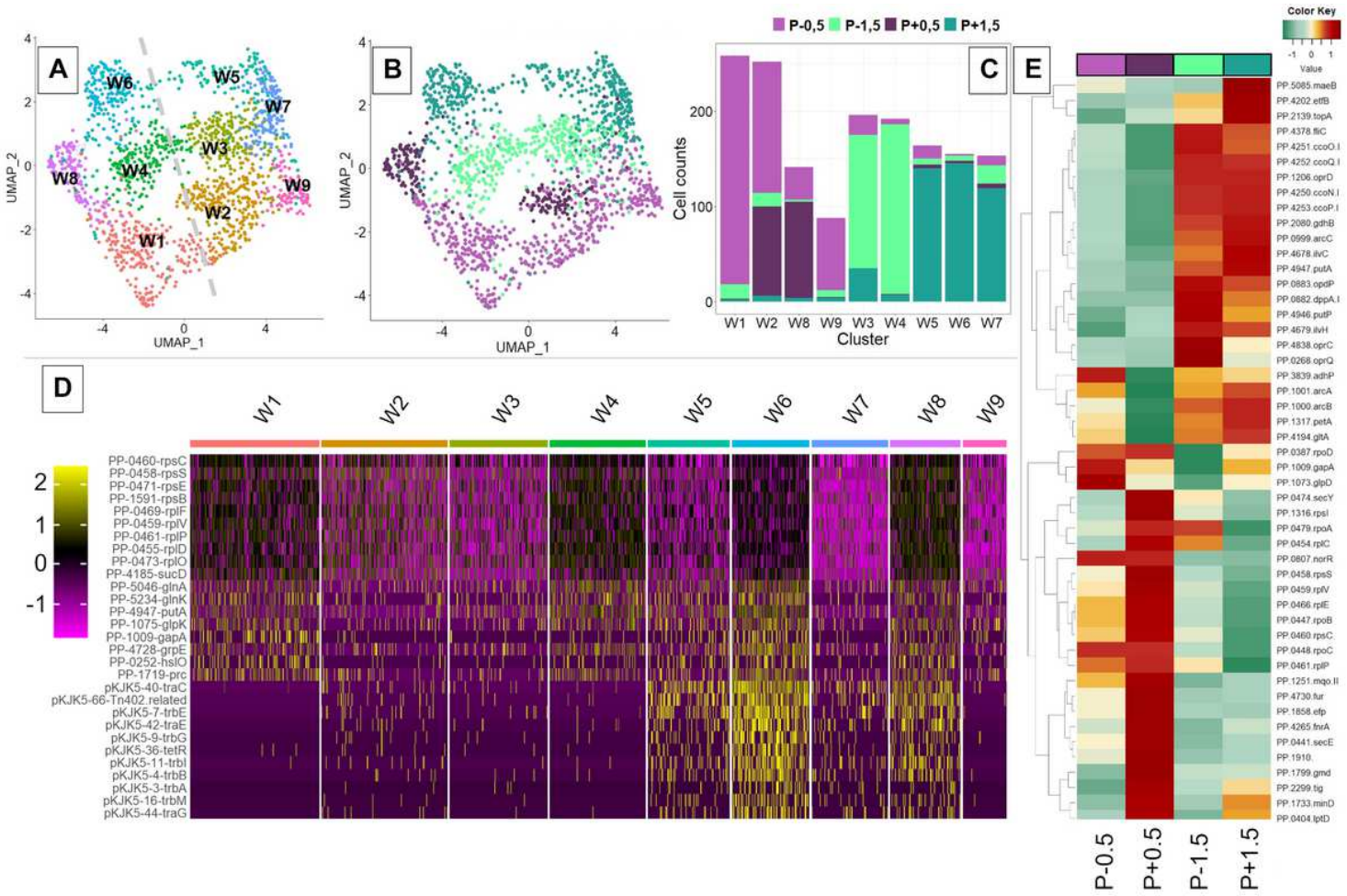

Figure 2

Whole single-cell transcriptomes generally cluster in accordance with growth state and the presence/absence of the plasmid. Subpopulation clustering identified by single-cell transcriptomics of P. putida carrying a plasmid (P+) or not (P-) at early (OD0.5) and late exponential growth (OD1.5). (A) UMAP obtained by microSPLiT scRNA sequencing identified 9 whole transcriptome clusters (W1-W9) where both plasmid and chromosomal transcripts were analyzed. The dashed line indicates cluster separation not linked to growth state or the presence/absence of plasmid. (B) Clusters segregate cell transcriptomes in subpopulations separating the two different growth states (OD0.5 and 1.5). (C) Cell transcriptomes from OD0.5 were mainly distributed in clusters W1, W2, W8 and W9, while cells from OD1.5 were mainly distributed in clusters W3-W7. (D) Heatmap of the normalized number of transcripts per cell. The top 10 biomarker genes identified by the Wilcoxon signed-rank test are shown for each cluster. (E) Heatmap obtained by averaging the normalized transcription of differentially expressed gene transcripts from the single-cell transcriptomes. Data from different growth states and the presence/absence of plasmids were grouped.

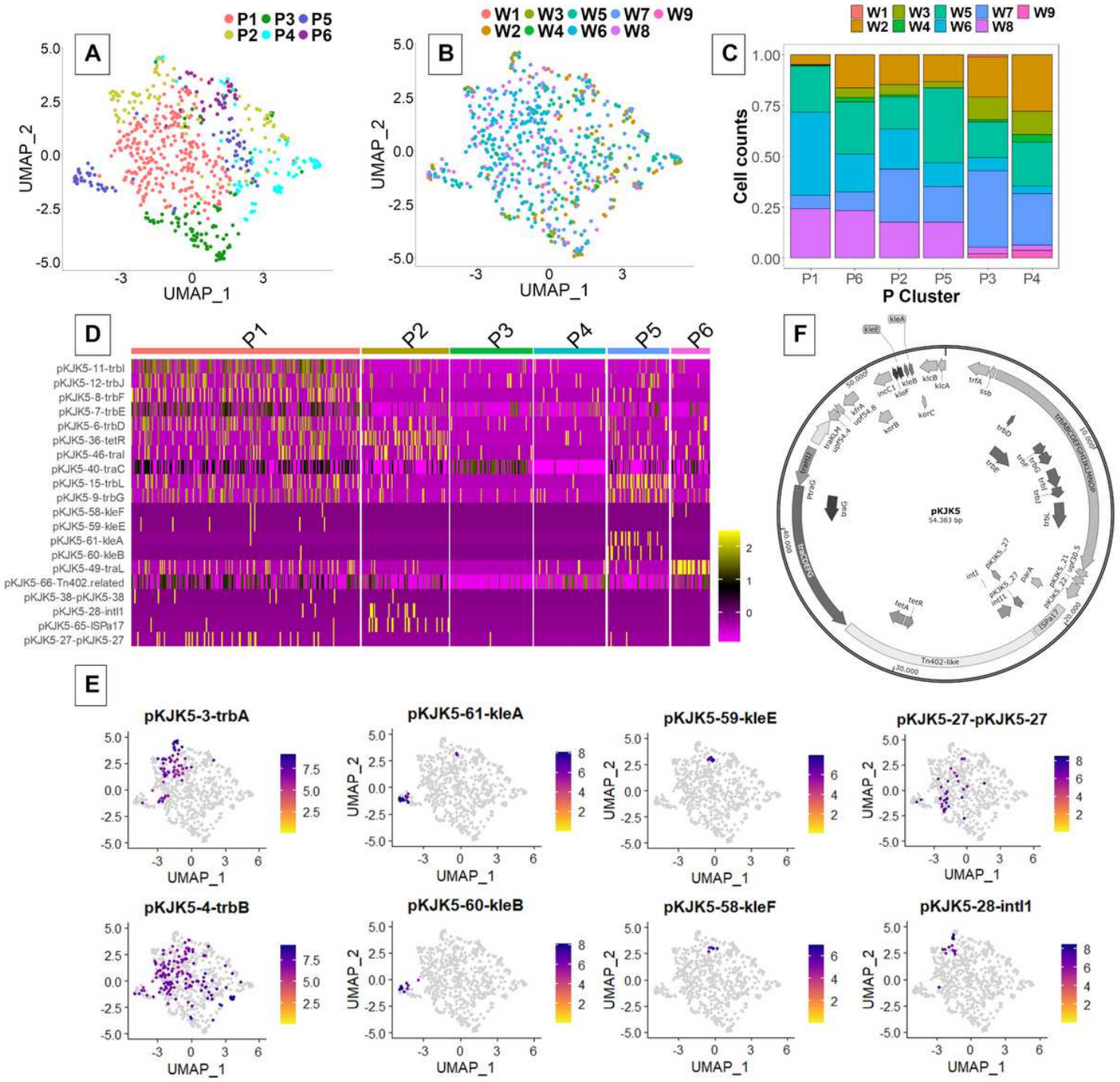

Figure 3

Plasmid single-cell transcriptome clustering suggests population heterogeneity in plasmid gene transcription, independent of growth state. Subpopulation clustering identified by single-cell transcriptomics of P. putida carrying the plasmid at early (OD0.5) and late exponential growth (OD1.5). (A) UMAP obtained by microSPLiT scRNA sequencing identified 6 plasmid transcriptome clusters (P1-P6) when only plasmid transcripts were analyzed. (B) Dots representing single-cell plasmid transcriptomes overlaid with colors indicating whole transcriptome clusters (W1-9), as shown in Figure 2A. (C) Normalized distribution of whole-cell transcriptomes within the six different clusters found based on

plasmid single-cell transcriptomes. (D) Heatmap of the normalized number of transcripts per cell ordered according to clusters P1-6. (E) Normalized transcript counts of selected genes from individual cells displayed on top of the UMAP generated with the plasmid single-cell transcriptomes. (F) Genome map of the pKJK5 plasmid made with SnapGene.

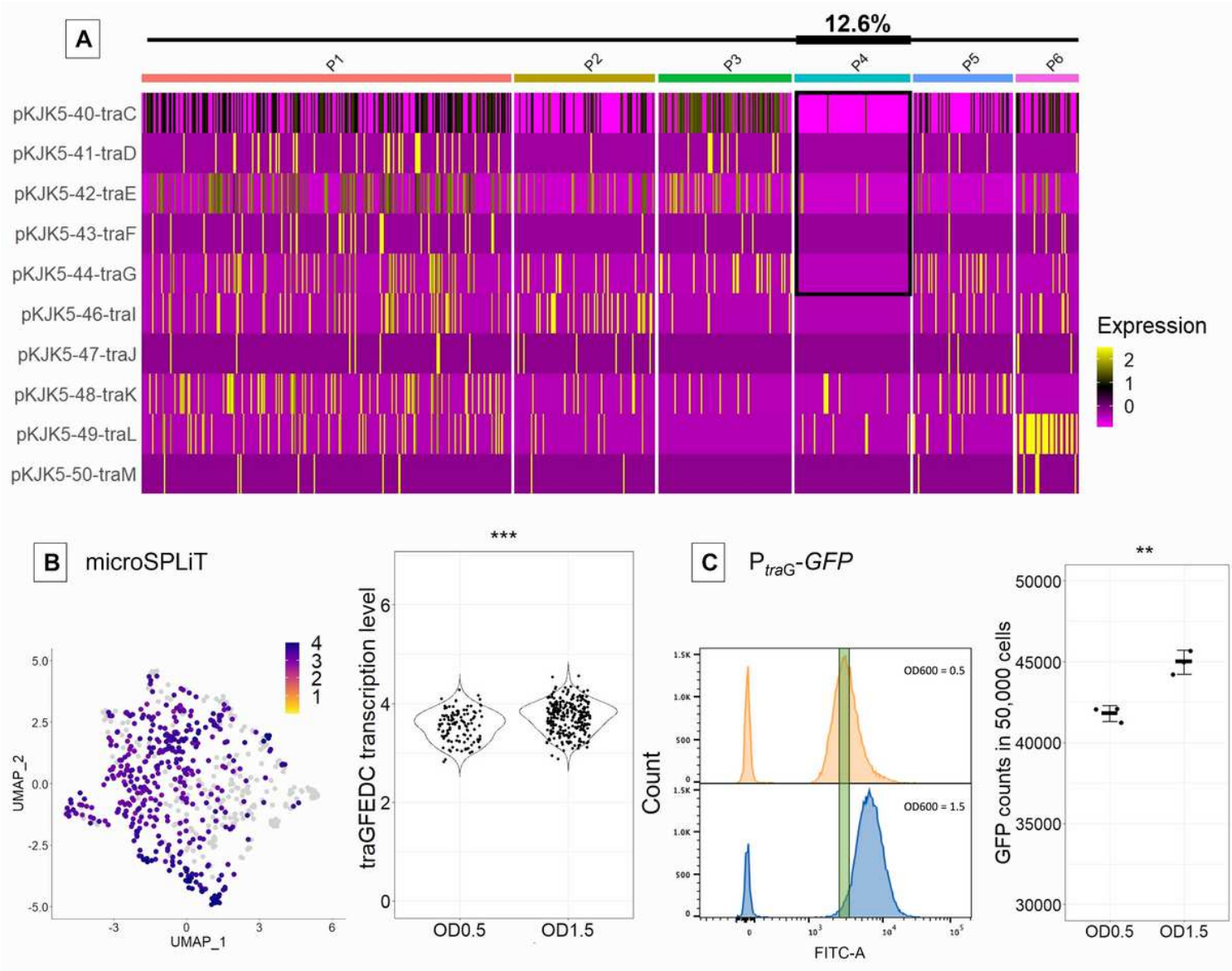

Figure 4

Subpopulation transcriptional heterogeneity of the traGFEDC operon, which is essential for conjugation, validated by flow cytometry of the promoter-sfGFP fusion reporter. (A) Heatmap of the normalized number of tra gene transcripts per cell ordered according to clusters P1-6. (B) Normalized summed transcript counts of traGFEDC genes from individual cells displayed on top of the UMAP generated with the plasmid single-cell transcriptomes and on a violin plot according to OD. (C) Flow cytometry histogram for PtraG-sfGFP signal and GFP cell counts from samples taken at OD0.5 and OD1.5.

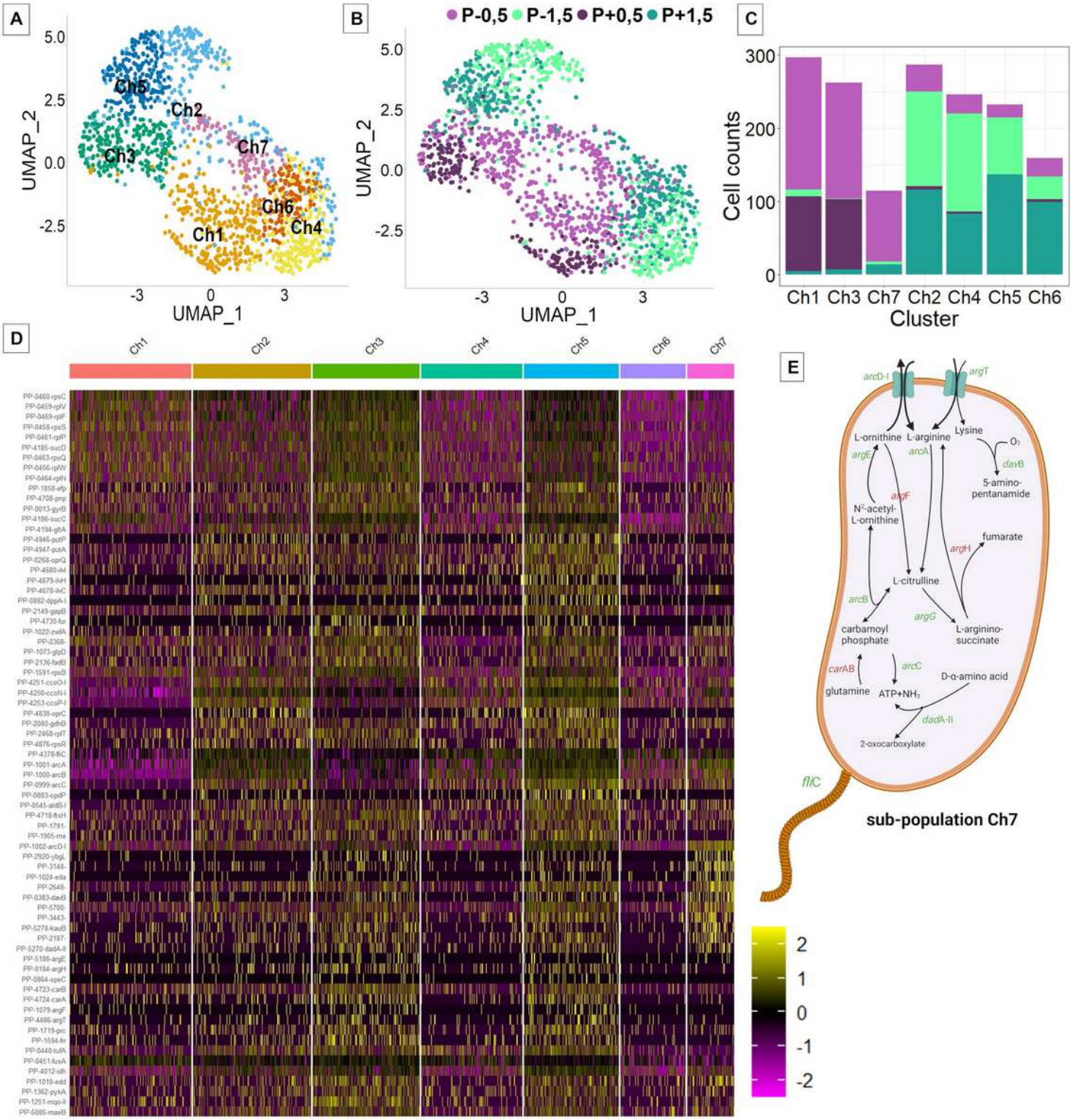

Figure 5

Chromosome single-cell transcriptomes generally cluster in accordance with growth state, yet the subpopulation dynamics are influenced by plasmid carriage. Subpopulation clustering identified by single-cell transcriptomics of Pseudomonas putida carrying the plasmid (P+) or not (P-) at early (OD0.5) and late exponential growth (OD1.5). Only chromosomal gene transcripts were analyzed. (A) UMAP of transcriptomes of P. putida obtained with microSPLiT RNA sequencing, identifying 7 (Ch1-Ch7) clusters.

(B) Clusters segregate cell transcriptomes in subpopulations separating the 2 different growth states (OD0.5 and 1.5). (C) Cell transcriptomes from OD0.5 were mainly distributed in clusters Ch1, Ch3 and Ch7, while cells from OD1.5 were mainly distributed in clusters Ch2, Ch4, Ch5 and Ch7. (D) Heatmap of biomarker genes of the different Ch clusters. An exhaustive heatmap can be found in Fig S11. (E) Schematic representation of upregulated (green) or downregulated (red) 457 genes in cells from cluster Ch7. Created with BioRender.com.

Supplementary Files

This is a list of supplementary files associated with this preprint. Click to download.

- SupplementaryinformationCyriaqueal.pdf